

# Iterative Identification and Control Using Non-normalized Coprime Factors With Application in Wafer Stage Motion Control

Frank Boeren<sup>1</sup>, Alexander Lanzon, and Tom Oomen

**Abstract**—Robustness against model uncertainty is essential in model-based controller design. It is well known that a relatively small uncertainty in lightly damped poles and zeros can result in a large distance measured in the  $\nu$ -gap metric, leading to conservative robust stability and performance guarantees. This paper aims to develop an identification and control procedure that results in less conservative robust stability and performance conditions for linear systems with lightly damped poles and zeros. To achieve this, a connection is established between a distance measure based on a nonnormalized coprime factorization of the system and existing identification criteria in closed-loop system identification. A nominal model of the system is determined by minimizing this distance measure by means of a frequency-domain identification algorithm. Then, a controller synthesis method is proposed that addresses both nominal performance as robust stability. Improved robustness by using the proposed approach compared to existing approaches is confirmed in an experimental example for a system with lightly damped poles and zeros.

**Index Terms**—Mechatronics, motion control, robust control, system identification.

## I. INTRODUCTION

**R**OBUSTNESS against model uncertainty is essential in feedback control, and as a consequence, determining the extent of model uncertainty is also necessary for the associated modeling technique. In identification for control, the only purpose of the identified linear model  $\hat{P}$  is to design a high-performance controller  $C$ . When implementing the controller  $C$  on the true (linear) system  $P_0$ , stability and performance cannot be guaranteed based on only the nominal model. Hence, a minimal requirement is that  $C$  achieves robust stability for a given model uncertainty set.

Manuscript received February 28, 2017; revised January 29, 2018 and June 22, 2018; accepted October 14, 2018. Date of publication December 4, 2018; date of current version February 14, 2020. Manuscript received in final form October 16, 2018. This work was supported in part by Philips Innovation Services, in part by the Engineering and Physical Sciences Research Council under Grant EP/R008876/1, and in part by the Netherlands Organisation for Scientific Research through the Research Programme VIDI under Project 15698. All research data supporting this publication are directly available within this publication. Recommended by Associate Editor R. Tóth. (Corresponding author: Alexander Lanzon.)

F. Boeren and T. Oomen are with the Control Systems Technology Group, Department of Mechanical Engineering, Eindhoven University of Technology, 5600 MB Eindhoven, The Netherlands (e-mail: f.a.j.boeren@tue.nl; t.a.e.oomen@tue.nl).

A. Lanzon is with the Control Systems Centre, School of Electrical and Electronic Engineering, University of Manchester, Manchester M13 9PL, U.K. (e-mail: alexander.lanzon@manchester.ac.uk).

Color versions of one or more of the figures in this article are available online at <http://ieeexplore.ieee.org>.

Digital Object Identifier 10.1109/TCST.2018.2877680

This is well recognized in identification for control, where such requirements are at the basis of iterative identification and control approaches [1]–[5].

Several approaches have been developed to analyze the influence of model uncertainty on the stability and performance of a closed-loop system. For example, robustness results can be derived by measuring the distance between systems, as originally introduced in the graph metric [6], gap metric [7], [8], and  $\nu$ -gap metric [9]. These approaches consider the discrepancy between systems around a normalized coprime factorization of the nominal model  $\hat{P}$  to derive robust stability and performance theorems, see [9, Sec. 3.3] for results in the  $\nu$ -gap. In [4], an iterative identification and control approach is proposed where the identification criterion is the  $\nu$ -gap metric, and the control criterion is the four-block performance measure used in  $\mathcal{H}_\infty$  loop-shaping [10]. The associated robust stability results are used to quantify the allowable controller modifications and model adjustments. Furthermore, a model reduction based on the  $\nu$ -gap metric is presented in [11].

The  $\nu$ -gap metric has important advantages in view of robust stability analysis compared to the graph and gap metric, yet, it has been shown in [12] and [13] that a relatively small uncertainty in lightly damped zeros and poles can result in a large distance in the  $\nu$ -gap. Uncertainty in lightly damped zeros and poles frequently occurs in mechanical systems, see [14]–[16]. A large distance measured in the  $\nu$ -gap results in a robust stability condition that is overly conservative [12], [17]. Thus, the  $\nu$ -gap may not be the most suitable distance measure for robust stability and robust performance in uncertain lightly damped systems.

Recently, it is shown in [12] that by relaxing the normalization condition on the coprime factors of  $\hat{P}$ , which is inherently at the basis of the  $\nu$ -gap, less conservative robust stability and performance guarantees can be determined for lightly damped systems. Essentially, by relaxing the normalization condition, additional freedom is introduced to tailor the uncertainty weighting. In particular, the additional freedom reduces conservatism by allowing for an improved frequency weighting and improved channel direction scaling of the uncertainty [12, Sec. X], [18, Sec. I]. The nonnormalized coprime factor uncertainty structure is embedded in the distance measure framework of [12], where robust stability and robust performance theorems are proposed for many standard uncertainty structures. Controller synthesis methods

that exploit nonnormalized coprime factorizations are presented in [17] and [19].

However, these approaches [12], [17], [19] assume that models of  $\hat{P}$  and  $P_0$  are readily available. Hence, despite the potential advantages of nonnormalized coprime factorizations in view of robust stability and robust performance, these methods cannot directly be applied if models of  $\hat{P}$  and  $P_0$  are not yet available. One of the aims of this paper is to develop an identification for control approach that is tailored to the general distance measure framework. Specifically, an identification procedure will be developed based on a nonnormalized coprime factor uncertainty structure that is particularly suitable for lightly damped systems.

The focus on normalized coprime factorizations in robust control has led to a focus on identifying normalized coprime factorizations in identification for control [3], [20]–[23]. Often, identification for control approaches utilizes the dual-Youla uncertainty structure of all plants that are stabilized by a known controller  $C^{\text{exp}}$  used during an identification experiment [2], [24]. Typically, a normalized coprime factorization of  $\hat{P}$  is used [25]. Interestingly, the potential of non-normalized coprime factorizations in identification for control is also explored in [18], where a particular nonnormalized coprime factorization of  $\hat{P}$  is introduced in a dual-Youla uncertainty structure to achieve a certain level of robust performance and reduce conservatism in subsequent  $\mu$ -synthesis. However,  $\mu$ -synthesis involves a nonconvex optimization and typically introduces additional conservatism [26]. The aim of this paper is to take a different approach based on nonnormalized coprime factorizations by building on  $\mathcal{H}_\infty$ -loop-shaping synthesis and  $\nu$ -gap analysis, both of which only consider normalized coprime factorizations.

The main contribution of this paper is a new framework for identification and control, which is particularly suited for lightly damped systems. The key point is that any identified model is an inexact representation of the true system. Although there are many ways of measuring the identification error, the interesting question is how to measure identification error in a specific way that can be used to synthesize a controller that *a priori* guarantees robust stability and a level of robust performance. The developed new framework substantially differs from existing mainstream robust control design frameworks. On the one hand, it extends the  $\mathcal{H}_\infty$ -loop-shaping and  $\nu$ -gap framework, e.g., [9], toward the use of nonnormalized coprime factorizations and compatible system identification techniques. On the other hand, it takes a fundamentally different approach compared to commonly used  $\mu$ -synthesis by avoiding such a nonconvex optimization. The focus of this paper is on the choice of uncertainty structure, not on quantification of the size of the uncertainty itself, which is only briefly touched upon in Section V of this paper. The following specific technical subcontributions are in this paper.

*C1:* Development of new results on traditional dual-Youla structures in a general framework that characterize a stability margin when a controller is changed and that characterize the associated robust performance degradation,

which will form the basis for the controller design approach developed in this paper.

*C2:* Development of a new measure on identification error based on a distance that is compatible with the aforementioned stability margin, and the development of a subsequent optimal identification algorithm. In addition, it is shown how this newly developed distance captures criteria used in prior identification literature [22], providing a theoretical foundation for those earlier results in terms of a distance framework.

*C3:* A compatible controller synthesis approach is developed that addresses robust performance, which is subsequently embedded in an overall identification and control design procedure.

*C4:* A case study on an industrial wafer stage system is performed, confirming a substantial improvement in performance. In addition, a thorough comparison of the proposed nonnormalized factorization methodology with existing normalized factorization techniques reveals that the proposed approach provides a guarantee for robust performance, while existing techniques provide none.

An outline of this paper is as follows. In Section II, the notation is introduced and background information is provided. In Section III, Contribution C1 is provided. Next, in Section IV, Contribution C2 is contained, followed by Contribution C3 in Section V. Then, in Section VI, an experimental case study on the wafer stage is provided, constituting Contribution C4. Conclusions are provided in Section VII.

## II. GENERAL DISTANCE MEASURE FRAMEWORK

### A. Notation

Throughout linear and time-invariant systems are considered. The set of proper real-rational transfer functions is denoted as  $\mathcal{R}$ . Let  $\mathcal{RL}_\infty$  denote the space of proper real-rational transfer functions bounded on  $j\mathbb{R}$  including  $\infty$ , and  $\mathcal{RH}_\infty$  denote the space of proper real-rational transfer functions bounded and analytic in the open right half-complex plane. For  $P \in \mathcal{R}$ ,  $\|P\|_\infty = \max_{\omega \in \mathbb{R} \cup \infty} \bar{\sigma}(P(j\omega))$ . The winding number  $\text{wno } p(s)$  of a scalar  $p(s)$  is defined as the number of encirclements of the origin made by  $p(s)$  as  $s$  follows the standard Nyquist D-contour, indented into the right half-plane (RHP) around any imaginary axis poles of  $p(s)$ . An upper linear fractional transformation (LFT) is given by  $\mathcal{F}_u(H, \Delta) = H_{22} + H_{21}\Delta(I - H_{11}\Delta)^{-1}H_{12}$ , and a lower LFT by  $\mathcal{F}_l(H, C) = H_{11} + H_{12}C(I - H_{22}C)^{-1}H_{21}$ . Throughout this paper,  $s = j\omega$ , where  $\omega \in \mathbb{R}$  denotes a frequency. Furthermore,  $\mathbb{R}[s]^{p \times q}$  denotes a polynomial matrix of dimension  $p \times q$  with real coefficients.

The pair  $\{N, M\}$  denotes a right coprime factorization (rcf) of  $P \in \mathcal{R}$  if  $M$  is invertible in  $\mathcal{R}$ ,  $N, M \in \mathcal{RH}_\infty$ ,  $P = NM^{-1}$ , and  $\exists X_r, Y_r \in \mathcal{RH}_\infty$  such that the Bezout identity  $X_rM + Y_rN = I$  holds. The pair  $\{N, M\}$  is a normalized rcf of a plant  $P$  if  $\{N, M\}$  is a rcf and  $M^*M + N^*N = I$ , where  $M^* = M(-s)^T$ . Dual definitions hold for a left coprime factorization (lcf), where  $P = \tilde{M}^{-1}\tilde{N}$  denotes a lcf of  $P$ . Furthermore,  $\{U, V\}$  denotes a rcf of a controller  $C$ , while  $\{\tilde{U}, \tilde{V}\}$  denotes a lcf of a controller  $C$ . Define  $G = \begin{bmatrix} N \\ M \end{bmatrix}$ ,

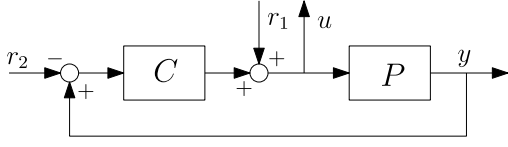


Fig. 1. Feedback interconnection.

$\tilde{G} = [-\tilde{M} \ \tilde{N}]$ , as the right and left graph symbols of  $P$ , respectively, and  $K = \begin{bmatrix} V \\ U \end{bmatrix}$ ,  $\tilde{K} = [-\tilde{U} \ \tilde{V}]$ , as the right and left inverse graph symbol of  $C$ . Here,  $\tilde{G}G = 0$  and  $\tilde{K}K = 0$  [9, (2.13)].

### B. Control Setup

Let  $[P, C]$  denote the positive feedback interconnection in Fig. 1, where  $P \in \mathcal{R}^{n_y \times n_u}$  denotes the plant and  $C \in \mathcal{R}^{n_u \times n_y}$  denotes the feedback controller. Here

$$\begin{bmatrix} y \\ u \end{bmatrix} = \begin{bmatrix} P \\ I \end{bmatrix} (I - CP)^{-1} \begin{bmatrix} -C & I \end{bmatrix} \begin{bmatrix} r_2 \\ r_1 \end{bmatrix}.$$

Furthermore, define  $T(P, C)$  as

$$T(P, C) = \begin{bmatrix} P \\ I \end{bmatrix} (I - CP)^{-1} \begin{bmatrix} -C & I \end{bmatrix}.$$

Then,  $[P, C]$  is internally stable if  $(I - CP)^{-1} \in \mathcal{R}$  and  $T(P, C) \in \mathcal{RH}_\infty$ . Furthermore, let  $\hat{P} \in \mathcal{R}^{n_y \times n_u}$  denote a nominal model of an unknown true plant  $P_0 \in \mathcal{R}^{n_y \times n_u}$ .

A model-based control approach is adopted to determine a controller  $C$ , where performance and robustness requirements are specified by means of the weighting scheme from [27]. This scheme is to precompensate and postcompensate  $\hat{P}$  and  $P_0$  with weighting functions  $W_1$  and  $W_2$ , respectively. The strictly proper shaped nominal model and shaped true plant become  $\hat{P}_s = W_2 \hat{P} W_1$  and  $P_{0,s} = W_2 P_0 W_1$ , respectively, while the shaped controller is given by  $C_s = W_1^{-1} C W_2^{-1}$ . Furthermore, the weighted feedback interconnection is considered, as denoted by  $[\hat{P}_s, C_s]$  and  $[P_{0,s}, C_s]$ . The stabilizing feedback controller that is used during a closed-loop identification experiment is denoted by  $C_s^{\text{exp}}$ . Thus,  $[P_{0,s}, C_s^{\text{exp}}]$  is assumed internally stable.

Let  $\{\tilde{N}_s, \tilde{M}_s\}$  be a lcf of  $\hat{P}_s$ , with left graph symbol  $\tilde{G}_s$  as defined in Section II-A. Furthermore,  $\{N_{0,s}, M_{0,s}\}$  is a rcf of  $P_{0,s}$ , while  $\{\tilde{N}_{0,s}, \tilde{M}_{0,s}\}$  is a lcf of  $P_{0,s}$ . The corresponding right and left graph symbols are  $G_{0,s}$  and  $\tilde{G}_{0,s}$ , respectively. Furthermore,  $\{\tilde{U}_s^{\text{exp}}, \tilde{V}_s^{\text{exp}}\}$  is a lcf of  $C_s^{\text{exp}}$ , while  $\{U_s, V_s\}$  is a rcf of  $C_s$ . The corresponding left and right inverse graph symbols are  $\tilde{K}_s^{\text{exp}}$  and  $K_s$ , respectively.

Finally, let the standard linear fractional interconnection in Fig. 2 is denoted by  $\langle H, C_s \rangle$ , with the generalized plant

$$H = \left[ \begin{array}{c|c} H_{11} & H_{12} \\ \hline H_{21} & H_{22} \end{array} \right] \in \mathcal{R}$$

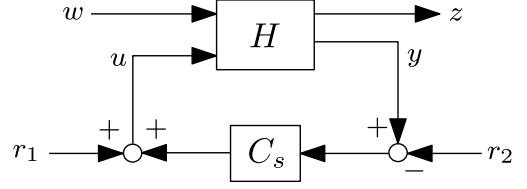


Fig. 2. Standard linear fractional interconnection.

and transfer function mapping  $\begin{bmatrix} w \\ r_2 \\ r_1 \end{bmatrix}$  to  $\begin{bmatrix} z \\ y \\ u \end{bmatrix}$  given in (1), as shown at the bottom of this page. The generalized plant is a widely adopted formulation that encompasses a large range of control problems and distance metrics, see [9] and [26] for details. Finally,  $H$  is said to be stabilizable if there exists a  $C_s$  such that  $\langle H, C_s \rangle$  is internally stable, that is, the transfer function in (1) belongs to  $\mathcal{RH}_\infty$ .

### C. General Distance Measure Framework

In this paper, robust stability and performance theorems are proposed according to the general distance measure framework in [12] and [28]. This framework is based on a generic distance measure  $d^H(\hat{P}_s, P_{0,s})$  and a generic robust stability margin  $b^H(\hat{P}_s, C_s)$ , as are defined next.

*Definition 1* [12, Definition 4]: Let a nominal model be given by  $\hat{P}_s \in \mathcal{R}^{n_y \times n_u}$ , a generalized plant by  $H \in \mathcal{R}$  with  $H_{22} = \hat{P}_s$ , and a true plant by  $P_{0,s} \in \mathcal{R}^{n_y \times n_u}$ . Let the set of all admissible perturbations be given by

$$\Delta = \{ \Delta_s \in \mathcal{RL}_\infty : (I - H_{11} \Delta_s)^{-1} \in \mathcal{R}, P_{0,s} = \mathcal{F}_u(H, \Delta_s) \}.$$

The distance measure  $d^H(\hat{P}_s, P_{0,s})$  between  $\hat{P}_s$  and  $P_{0,s}$  for the uncertainty structure implied by  $H$  is defined as

$$d^H(\hat{P}_s, P_{0,s}) = \begin{cases} \inf_{\Delta_s \in \Delta} \|\Delta_s\|_\infty, & \text{if } \Delta \neq \emptyset \\ \infty, & \text{otherwise.} \end{cases}$$

Note that  $d^H(\hat{P}_s, P_{0,s}) \geq 0$  and  $d^H(\hat{P}_s, \hat{P}_s) = 0$ . The counterpart of the distance measure  $d^H(\hat{P}_s, P_{0,s})$  in robust stability and performance analysis is the robust stability margin  $b^H(\hat{P}_s, C_s)$  of  $\langle H, C_s \rangle$ .

*Definition 2* [12, Definition 3]: Let a nominal model be given by  $\hat{P}_s \in \mathcal{R}^{n_y \times n_u}$ , a generalized plant by  $H \in \mathcal{R}$  with  $H_{22} = \hat{P}_s$ , and a controller by  $C_s \in \mathcal{R}^{n_u \times n_y}$ . The robust stability margin  $b^H(\hat{P}_s, C_s)$  for the uncertainty structure implied by  $H$  is defined as

$$b^H(\hat{P}_s, C_s) = \begin{cases} \|\mathcal{F}_l(H, C_s)\|_\infty^{-1}, & \text{if } 0 \neq \mathcal{F}_l(H, C_s) \in \mathcal{RL}_\infty \text{ and} \\ & [\hat{P}_s, C_s] \text{ is internally stable} \\ 0, & \text{otherwise.} \end{cases}$$

Within the general distance measure framework, specific expressions for  $d^H(\hat{P}_s, P_{0,s})$  and  $b^H(\hat{P}_s, C_s)$  are

$$\begin{bmatrix} z \\ y \\ u \end{bmatrix} = \left[ \begin{array}{c|c} \mathcal{F}_l(H, C_s) & H_{12}(I - C_s H_{22})^{-1} \begin{bmatrix} -C_s & I \end{bmatrix} \\ \hline \begin{bmatrix} H_{21} \\ 0 \end{bmatrix} + \begin{bmatrix} H_{22} \\ I \end{bmatrix} (I - C_s H_{22})^{-1} C_s H_{21} & \begin{bmatrix} H_{22} \\ I \end{bmatrix} (I - C_s H_{22})^{-1} \begin{bmatrix} -C_s & I \end{bmatrix} \end{array} \right] \begin{bmatrix} w \\ r_2 \\ r_1 \end{bmatrix} \quad (1)$$

derived in [12] for the commonly used uncertainty structures listed in [29, Table 9.1]. These expressions are presented in [12, Table II].

### III. ROBUST STABILITY AND ROBUST PERFORMANCE GUARANTEES FOR A DUAL-YOULA UNCERTAINTY STRUCTURE

In this section, the dual-Youla uncertainty structure, as often used in identification for control [25], [30], is embedded in the general distance measure framework described in Section II-C. The dual-Youla representation has the form

$$P_{0,s} = (\tilde{M}_s + \Delta_s \tilde{U}_s^{\text{exp}})^{-1} (\tilde{N}_s + \Delta_s \tilde{V}_s^{\text{exp}}) \quad (2)$$

where  $(\tilde{M}_s + \Delta_s \tilde{U}_s^{\text{exp}})^{-1} \in \mathcal{R}$ . In view of the technical machinery used in the general distance measure framework, (2) is in the rest of this paper represented as  $P_{0,s} = \mathcal{F}_u(H, \Delta_s)$  [under the assumption that  $(I - H_{11}\Delta_s)^{-1} \in \mathcal{R}$ ], with generalized plant  $H$  given by

$$H = \left[ \begin{array}{c|c} -\tilde{U}_s^{\text{exp}} \tilde{M}_s^{-1} & \tilde{V}_s^{\text{exp}} - \tilde{U}_s^{\text{exp}} \hat{P}_s \\ \hline \tilde{M}_s^{-1} & \hat{P}_s \end{array} \right] \quad (3)$$

and (unstructured) uncertainty block  $\Delta \in \mathcal{RL}_{\infty}^{n_y \times n_u}$ .

Note that  $H$  in (3) depends via the lcf  $\{\tilde{U}_s^{\text{exp}}, \tilde{V}_s^{\text{exp}}\}$  on the known stabilizing controller  $C_s^{\text{exp}}$  as used in an identification experiment on  $[P_{0,s}, C_s^{\text{exp}}]$ . Clearly,  $[P_{0,s}, C_s^{\text{exp}}]$  is internally stable. Furthermore, it is assumed that  $\hat{P}_s$  is determined such that  $[\hat{P}_s, C_s^{\text{exp}}]$  is also internally stable.

Given  $H$  in (3), a distance measure  $d^Y(\hat{P}_s, P_{0,s})$  and robust stability margin  $b^Y(\hat{P}_s, C_s)$  will be derived in Section III-A based on  $d^H(\hat{P}_s, P_{0,s})$  in Definition 1 and  $b^H(\hat{P}_s, C_s)$  in Definition 2. These results extend [12, Table II] toward the dual-Youla uncertainty structure. Then, in Section III-B, robust stability and performance conditions are formulated based on  $d^Y(\hat{P}_s, P_{0,s})$  and  $b^Y(\hat{P}_s, C_s)$ . These conditions are essential for the identification approach in Section IV and the controller synthesis method in Section V.

#### A. Distance Measure and Robust Stability Margin

To determine  $d^Y(\hat{P}_s, P_{0,s})$  according to Definition 1, all solutions  $\Delta_s \in \mathcal{RL}_{\infty}$  should be determined that satisfy the consistency of equations condition, i.e.,  $P_{0,s} = \mathcal{F}_u(H, \Delta_s)$ , and the well-posedness condition  $(I - H_{11}\Delta_s)^{-1} \in \mathcal{R}$ . By assuming that  $(I - H_{11}\Delta_s)^{-1} \in \mathcal{R}$ , all  $\Delta_s \in \mathcal{RL}_{\infty}$  that satisfy  $P_{0,s} = \mathcal{F}_u(H, \Delta_s)$  for given  $\hat{P}_s, P_{0,s}$ , and  $C_s^{\text{exp}}$  can be determined as follows:

$$\begin{aligned} P_{0,s} &= \mathcal{F}_u(H, \Delta_s) \\ &= \hat{P}_s + \tilde{M}_s^{-1} \Delta_s (I + \tilde{U}_s^{\text{exp}} \tilde{M}_s^{-1} \Delta_s)^{-1} (\tilde{V}_s^{\text{exp}} - \tilde{U}_s^{\text{exp}} \hat{P}_s) \\ &\Leftrightarrow P_{0,s} - \hat{P}_s = (\tilde{M}_s + \Delta_s \tilde{U}_s^{\text{exp}})^{-1} \Delta_s (\tilde{V}_s^{\text{exp}} - \tilde{U}_s^{\text{exp}} \hat{P}_s) \\ &\Leftrightarrow (\tilde{M}_s + \Delta_s \tilde{U}_s^{\text{exp}})(P_{0,s} - \hat{P}_s) = \Delta_s (\tilde{V}_s^{\text{exp}} - \tilde{U}_s^{\text{exp}} \hat{P}_s) \\ &\Leftrightarrow \tilde{M}_s (P_{0,s} - \hat{P}_s) = \Delta_s (\tilde{V}_s^{\text{exp}} - \tilde{U}_s^{\text{exp}} P_{0,s}) \\ &\Leftrightarrow (\tilde{M}_s N_{0,s} - \tilde{N}_s M_{0,s}) = \Delta_s (\tilde{V}_s^{\text{exp}} M_{0,s} - \tilde{U}_s^{\text{exp}} N_{0,s}) \\ &\Leftrightarrow -\tilde{G}_s G_{0,s} = \Delta_s (\tilde{K}_s^{\text{exp}} G_{0,s}) \\ &\Leftrightarrow \Delta_s = -\tilde{G}_s G_{0,s} (\tilde{K}_s^{\text{exp}} G_{0,s})^{-1} \end{aligned} \quad (4)$$

which reveals that for  $H$  in (3), a unique solution  $\Delta_s$  always exists for  $P_{0,s} = \mathcal{F}_u(H, \Delta_s)$  [under the assumption that  $(I - H_{11}\Delta_s)^{-1} \in \mathcal{R}$ ]. Furthermore, since  $[P_{0,s}, C_s^{\text{exp}}]$  is internally stable  $\Leftrightarrow (\tilde{K}_s^{\text{exp}} G_{0,s})^{-1} \in \mathcal{RH}_{\infty}$ , see, [9, Proposition 1.9], it follows from (4) that  $\Delta_s \in \mathcal{RH}_{\infty}$ , as is indeed demanded via the Youla parametrization.

Next, the well-posedness condition  $(I - H_{11}\Delta_s)^{-1} \in \mathcal{R}$  is checked. Substituting (3) and (4) into  $(I - H_{11}\Delta_s)^{-1}$  gives

$$\begin{aligned} (I - H_{11}\Delta_s)^{-1} &= (I - \tilde{U}_s^{\text{exp}} \tilde{M}_s^{-1} \tilde{G}_s G_{0,s} (\tilde{K}_s^{\text{exp}} G_{0,s})^{-1})^{-1} \\ &= \tilde{K}_s^{\text{exp}} G_{0,s} (\tilde{K}_s^{\text{exp}} G_{0,s} - \tilde{U}_s^{\text{exp}} \tilde{M}_s^{-1} \tilde{G}_s G_{0,s})^{-1} \\ &= \tilde{K}_s^{\text{exp}} G_{0,s} ((\tilde{K}_s^{\text{exp}} - \tilde{U}_s^{\text{exp}} [-I \ \hat{P}_s]) G_{0,s})^{-1} \\ &= \tilde{K}_s^{\text{exp}} G_{0,s} ((\tilde{V}_s^{\text{exp}} - \tilde{U}_s^{\text{exp}} \hat{P}_s) M_{0,s})^{-1} \\ &= \tilde{K}_s^{\text{exp}} G_{0,s} M_{0,s}^{-1} (\tilde{V}_s^{\text{exp}} - \tilde{U}_s^{\text{exp}} \hat{P}_s)^{-1} \\ &= (\tilde{V}_s^{\text{exp}} - \tilde{U}_s^{\text{exp}} P_{0,s}) (\tilde{V}_s^{\text{exp}} - \tilde{U}_s^{\text{exp}} \hat{P}_s)^{-1}. \end{aligned}$$

Consequently,  $(I - H_{11}\Delta_s)^{-1} \in \mathcal{R}$  is equivalent to

$$\begin{aligned} &(\tilde{V}_s^{\text{exp}} - \tilde{U}_s^{\text{exp}} P_{0,s}) (\tilde{V}_s^{\text{exp}} - \tilde{U}_s^{\text{exp}} \hat{P}_s)^{-1} \in \mathcal{R} \\ &\Leftrightarrow (\tilde{V}_s^{\text{exp}})^{-1} (\tilde{V}_s^{\text{exp}} - \tilde{U}_s^{\text{exp}} P_{0,s}) (\tilde{V}_s^{\text{exp}} - \tilde{U}_s^{\text{exp}} \hat{P}_s)^{-1} \tilde{V}_s^{\text{exp}} \in \mathcal{R} \\ &\Leftrightarrow (I - C_s^{\text{exp}} P_{0,s}) (I - C_s^{\text{exp}} \hat{P}_s)^{-1} \in \mathcal{R} \end{aligned}$$

which is trivially fulfilled since  $[\hat{P}_s, C_s^{\text{exp}}]$  is well posed.

Thus, given  $H$  in (3) and  $\Delta_s$  in (4),  $(I - H_{11}\Delta_s)^{-1} \in \mathcal{R}$  is always automatically guaranteed by the well-posedness assumption of  $[\hat{P}_s, C_s^{\text{exp}}]$  and there always exists a unique  $\Delta_s \in \mathcal{RH}_{\infty}$  such that  $P_{0,s} = \mathcal{F}_u(H, \Delta_s)$  holds. Straight from Definition 1, the solution set  $\mathbf{\Delta}$  becomes

$$\mathbf{\Delta} = \{\Delta_s = -\tilde{G}_s G_{0,s} (\tilde{K}_s^{\text{exp}} G_{0,s})^{-1} \in \mathcal{RH}_{\infty}\}$$

for a given  $\hat{P}_s, P_{0,s}$ , and  $C_s^{\text{exp}}$ . Note that  $\mathbf{\Delta}$  contains only one element, and that  $\Delta_s \in \mathcal{RH}_{\infty}$  rather than  $\mathcal{RL}_{\infty}$ . This considerably simplifies the robust stability and performance analysis, by eliminating the need for an additional condition on the winding numbers [9], [12]. For  $\Delta_s$  given in (4), it can be shown that  $\text{wno det}(I - H_{11}\Delta_s) = \text{wno det}[(\tilde{K}_s^{\text{exp}} G_s) M_s^{-1} M_{0,s} (\tilde{K}_s^{\text{exp}} G_{0,s})^{-1}] = \eta(P_{0,s}) - \eta(\hat{P}_s)$ . Hence,  $\eta(P_{0,s}) = \eta(\hat{P}_s) + \text{wno det}(I - H_{11}\Delta_s)$  is trivially fulfilled, where  $\eta(\cdot)$  is the number of RHP poles and the winding number is evaluated on a contour indented to the right around any imaginary axis poles of  $\hat{P}_s$  and  $P_{0,s}$ . Then, straight from Definition 1, it follows that the distance measure  $d^Y(\hat{P}_s, P_{0,s})$  for the dual-Youla uncertainty structure becomes

$$d^Y(\hat{P}_s, P_{0,s}) = \|\tilde{G}_s G_{0,s} (\tilde{K}_s^{\text{exp}} G_{0,s})^{-1}\|_{\infty}. \quad (5)$$

The robust stability margin  $b^Y(\hat{P}_s, C_s)$  can be determined by substituting  $\mathcal{F}_l(H, C_s)$  as given by

$$\begin{aligned} \mathcal{F}_l(H, C_s) &= (-\tilde{U}_s^{\text{exp}} + (\tilde{V}_s^{\text{exp}} - \tilde{U}_s^{\text{exp}} \hat{P}_s) C_s (I - \hat{P}_s C_s)^{-1}) \tilde{M}_s^{-1} \\ &= (-\tilde{U}_s^{\text{exp}} (I - \hat{P}_s C_s) + (\tilde{V}_s^{\text{exp}} - \tilde{U}_s^{\text{exp}} \hat{P}_s) C_s) (I - \hat{P}_s C_s)^{-1} \tilde{M}_s^{-1} \\ &= [-\tilde{U}_s^{\text{exp}} \ \tilde{V}_s^{\text{exp}}] \begin{bmatrix} I \\ C_s \end{bmatrix} (I - \hat{P}_s C_s)^{-1} \tilde{M}_s^{-1} \\ &= -\tilde{K}_s^{\text{exp}} K_s (\tilde{G}_s K_s)^{-1} \end{aligned}$$

in Definition 2. Then, it follows directly from Definition 2 that  $b^Y(\hat{P}_s, C_s)$  for the dual-Youla uncertainty structure is given by

$$b^Y(\hat{P}_s, C_s) = \begin{cases} \left\| \tilde{K}_s^{\text{exp}} K_s (\tilde{G}_s K_s)^{-1} \right\|_{\infty}^{-1}, & \text{if } C_s \neq C_s^{\text{exp}} \text{ and} \\ & [\hat{P}_s, C_s] \text{ is internally stable} \\ 0, & \text{otherwise.} \end{cases} \quad (6)$$

The condition  $0 \neq \mathcal{F}_l(H, C_s)$  in Definition 2 is satisfied if and only if  $C_s \neq C_s^{\text{exp}}$ . Note that robust stability is trivially satisfied for  $C_s = C_s^{\text{exp}}$ . Furthermore,  $\mathcal{F}_l(H, C_s) \in \mathcal{RL}_{\infty}$  is not required in (6), since internal stability of  $[\hat{P}_s, C_s]$  is equivalent to  $(\tilde{G}_s K_s)^{-1} \in \mathcal{RH}_{\infty}$  which in turn implies that  $\mathcal{F}_l(H, C_s) \in \mathcal{RH}_{\infty}$ .

In summary, a distance measure  $d^Y(\hat{P}_s, P_{0,s})$  and a robust stability margin  $b^Y(\hat{P}_s, C_s)$  are determined for the dual-Youla uncertainty structure in (2). Next, robust stability and performance theorems are proposed based on  $d^Y(\hat{P}_s, P_{0,s})$  in (5) and  $b^Y(\hat{P}_s, C_s)$  in (6).

### B. Robust Stability and Robust Performance

In this section, robust stability and robust performance theorems are proposed based on  $d^Y(\hat{P}_s, P_{0,s})$  in (5) and  $b^Y(\hat{P}_s, C_s)$  in (6). The robust stability theorem gives conditions for internal stability of  $[P_{0,s}, C_s]$  through an upper bound on  $d^Y(\hat{P}_s, P_{0,s})$ . In the robust performance theorem, the difference in the performance between  $[\hat{P}_s, C_s]$  and  $[P_{0,s}, C_s]$  is quantified using  $d^Y(\hat{P}_s, P_{0,s})$ ,  $b^Y(\hat{P}_s, C_s)$ , and  $b^Y(P_{0,s}, C_s)$ . First, a robust stability condition is proposed in Theorem 1. It can be seen that this theorem is a specialization of [12, Th. 1] to the dual-Youla uncertainty structure.

*Theorem 1 (Robust Stability):* Let  $\hat{P}_s \in \mathcal{R}^{n_y \times n_u}$ ,  $P_{0,s} \in \mathcal{R}^{n_y \times n_u}$ ,  $H$  in (3),  $C_s^{\text{exp}} \in \mathcal{R}^{n_u \times n_y}$ , and  $C_s \in \mathcal{R}^{n_u \times n_y}$ . Furthermore, let  $d^Y(\hat{P}_s, P_{0,s})$  be given by (5) and  $b^Y(\hat{P}_s, C_s)$  be given by (6). Then,  $[P_{0,s}, C_s]$  is internally stable if  $d^Y(\hat{P}_s, P_{0,s}) < b^Y(\hat{P}_s, C_s)$ .

*Proof:* If  $d^Y(\hat{P}_s, P_{0,s}) < b^Y(\hat{P}_s, C_s)$ , then  $b^Y(\hat{P}_s, C_s) > 0$ , and from (6), it follows that  $[\hat{P}_s, C_s]$  is internally stable and  $\mathcal{F}_l(H, C_s) \in \mathcal{RH}_{\infty}$ . By substituting  $H$  as given in (3) into (1) and using that  $\mathcal{F}_l(H, C_s) \in \mathcal{RH}_{\infty}$ , (1) implies that  $\langle H, C_s \rangle$  is internally stable. This shows that  $H$  is stabilizable.

Since  $H$  is stabilizable and  $[\hat{P}_s, C_s]$  is internally stable, it follows from the proof of [9, Lemma 1.22] that  $d^Y(\hat{P}_s, P_{0,s}) < b^Y(\hat{P}_s, C_s) \Rightarrow [P_{0,s}, C_s]$  is internally stable.  $\square$

Next, robust performance conditions are proposed in Theorem 2. To illustrate the connection between Theorem 2 and the generic robust stability and performance conditions in [12, Theorems 1 and 3], note that the conditions in [12] are based on a generalized plant  $H^{\text{gen}}$  expressed as

$$H^{\text{gen}} = \left[ \begin{array}{c|c} S_z & I \\ \hline I & \end{array} \right] \left[ \begin{array}{c|c} I & -\hat{P}_s \\ \hline 0 & I \\ \hline I & -\hat{P}_s \end{array} \middle| \begin{array}{c} \hat{P}_s \\ \hat{P}_s \end{array} \right] \left[ \begin{array}{c|c} S_w & I \\ \hline I & \end{array} \right]$$

with  $S_w, S_z \in \mathcal{R}$ , and  $H_0^{\text{gen}}$  as

$$H_0^{\text{gen}} = \left[ \begin{array}{c|c} S_z & I \\ \hline I & \end{array} \right] \left[ \begin{array}{c|c} I & -P_{0,s} \\ \hline 0 & 0 \\ \hline I & -P_{0,s} \end{array} \middle| \begin{array}{c} P_{0,s} \\ I \\ P_{0,s} \end{array} \right] \left[ \begin{array}{c|c} S_{w_0} & I \\ \hline I & \end{array} \right]$$

with  $S_{w_0} = S_w(I - k\Delta_s S_z S_w)^{-1} \in \mathcal{R}$  for a given  $k \in \{0, 1\}$ . The dual-Youla uncertainty structure with  $H$  in (3) and  $H_0$  in (8) will be generated by using  $k = 1$ ,  $S_z = \tilde{K}_s^{\text{exp}}$ , and  $S_w = \left[ \begin{array}{c} \tilde{M}_s^{-1} \\ 0 \end{array} \right]$ .

*Theorem 2 (Robust Performance):* Let the assumptions of Theorem 1 hold and furthermore suppose that  $d^Y(\hat{P}_s, P_{0,s}) < b^Y(\hat{P}_s, C_s)$ . Then

$$|b^Y(P_{0,s}, C_s) - b^Y(\hat{P}_s, C_s)| \leq d^Y(\hat{P}_s, P_{0,s}) \quad (7)$$

and

$$\|\mathcal{F}_l(H_0, C_s) - \mathcal{F}_l(H, C_s)\|_{\infty} \leq \frac{d^Y(\hat{P}_s, P_{0,s})}{b^Y(\hat{P}_s, C_s)b^Y(P_{0,s}, C_s)}$$

with  $H$  in (3) and

$$H_0 = \left[ \begin{array}{c|c} -\tilde{U}_s^{\text{exp}} \tilde{M}_{0,s}^{-1} & \tilde{V}_s^{\text{exp}} - \tilde{U}_s^{\text{exp}} P_{0,s} \\ \hline \tilde{M}_{0,s}^{-1} & P_{0,s} \end{array} \right]. \quad (8)$$

*Proof:* This theorem is a specialization of [12, Theorem 3] to the dual-Youla uncertainty structure using  $k = 1$ ,  $S_z = \tilde{K}_s^{\text{exp}}$ , and  $S_w = \left[ \begin{array}{c} \tilde{M}_s^{-1} \\ 0 \end{array} \right]$ .  $\square$

Concluding, robust stability and performance conditions are proposed for the dual-Youla uncertainty structure within the general distance framework outlined in Section II-C. This constitutes Contribution C1. Furthermore, the results in this section confirm the generality of the distance measure approach in [12].

Throughout this section, it was tacitly assumed that  $\hat{P}_s$ ,  $P_{0,s}$ , and  $C_s$  were known when evaluating the robust stability and performance conditions. This assumption is removed in the remaining of this paper. Only a frequency response function (FRF) of  $P_{0,s}$  is known beforehand. Then, the goal of the identification and control approach proposed in this paper is to determine  $C_s$  based on a to-be-identified model  $\hat{P}_s$  that achieves high robust performance, as precisely characterized in Theorem 2. Robust stability is a minimal requirement to achieve high robust performance. Therefore, the robust stability condition in Theorem 1 is at the basis of the proposed identification and control approach in this paper, similar to the identification and control approaches in [1]–[5]. In Section IV,  $\hat{P}_s$  is identified based on a FRF of  $P_{0,s}$  in view of the robust stability condition in Theorem 1.

## IV. IDENTIFICATION FOR CONTROL WITHIN THE GENERAL DISTANCE MEASURE FRAMEWORK

In this section, a nominal model  $\hat{P}_s$  is determined as a representation for the unknown true plant  $P_{0,s}$ . To this end, measured data are used that are obtained from a closed-loop identification experiment on  $[P_{0,s}, C_s^{\text{exp}}]$ . In view of the robust stability and performance conditions derived in Section III-B,

the following optimization problem is proposed to determine  $\hat{P}_s$ :

$$\min_{\hat{P}_s} d^Y(\hat{P}_s, P_{0,s}) \quad (9)$$

with  $d^Y(\hat{P}_s, P_{0,s})$  in (5). In Section IV-B, appropriate identification experiments on the unknown true system  $P_{0,s}$  are conducted to obtain a tractable optimization problem regarding (9). The only purpose of  $\hat{P}_s$  in an  $\mathcal{H}_\infty$  setting is to enable the synthesis of  $C_s$  that achieves high performance on  $[P_{0,s}, C_s]$ . Condition (7) shows that the performance in terms of  $b^Y(P_{0,s}, C_s)$  is comparable to  $b^Y(\hat{P}_s, C_s)$  if  $d^Y(\hat{P}_s, P_{0,s})$  is small and  $C_s$  achieves a robust stability margin  $b^Y(\hat{P}_s, C_s)$  greater than the distance measure  $d^Y(\hat{P}_s, P_{0,s})$ . Then, a controller  $C_s$  that achieves high nominal performance also achieves high performance on  $[P_{0,s}, C_s]$ . This is the motivation to consider (9) in the identification step of the proposed identification and control approach.

In Section IV-A, it is shown that the distance measure  $d^Y(\hat{P}_s, P_{0,s})$  in (5) depends on the particular choices of coprime factorizations of  $\hat{P}_s$  and  $C_s^{\text{exp}}$ . This freedom in coprime factorizations is exploited to propose a  $d^Y(\hat{P}_s, P_{0,s})$  that is connected to existing identification criteria in closed-loop system identification. Then, in Section IV-B, a frequency-domain algorithm is proposed to determine  $\hat{P}_s$  based on measured FRF data.

#### A. Identification for Control

In this section, the freedom in coprime factorizations of  $\hat{P}_s$  and  $C_s^{\text{exp}}$  is exploited to connect (9) to a closed-loop identification criterion. First, it is shown that  $d^Y(\hat{P}_s, P_{0,s})$  depends on the coprime factorizations of  $\hat{P}_s$  and  $C_s^{\text{exp}}$ .

Given a lcf  $\{\tilde{N}_s, \tilde{M}_s\}$  of  $\hat{P}_s$ , all possible lcf's of  $\hat{P}_s$  can be generated by  $\{Q\tilde{N}_s, Q\tilde{M}_s\}$ , where  $Q, Q^{-1} \in \mathcal{RH}_\infty$ . In the remainder of this section, any possible lcf of  $\hat{P}_s$  is related to a normalized lcf of  $\hat{P}_s$ . Let  $\{\tilde{N}_s, \tilde{M}_s\}$  be a normalized lcf of  $\hat{P}_s$  with corresponding normalized left graph symbol  $\tilde{G}_s$ . Then,  $\{\tilde{N}_s = Q_1\tilde{N}_s, \tilde{M}_s = Q_1\tilde{M}_s\}$  is a (not necessarily normalized) lcf of  $\hat{P}_s$  related to  $\{\tilde{N}_s, \tilde{M}_s\}$  via  $Q_1, Q_1^{-1} \in \mathcal{RH}_\infty$ , and left graph symbol  $\tilde{G}_s = Q_1\tilde{G}_s$ . Similarly, let  $\{\tilde{U}_s^{\text{exp}}, \tilde{V}_s^{\text{exp}}\}$  be a normalized lcf of  $C_s^{\text{exp}}$  with normalized left inverse graph symbol  $\tilde{K}_s^{\text{exp}}$ . Then,  $\tilde{K}_s^{\text{exp}} = Q_2\tilde{K}_s^{\text{exp}}$  with  $Q_2, Q_2^{-1} \in \mathcal{RH}_\infty$ . Using  $\tilde{G}_s = Q_1\tilde{G}_s$  and  $\tilde{K}_s^{\text{exp}} = Q_2\tilde{K}_s^{\text{exp}}$  in (5) gives

$$d^Y(\hat{P}_s, P_{0,s}) = \|Q_1\tilde{G}_s\tilde{G}_{0,s}(\tilde{K}_s^{\text{exp}}\tilde{G}_{0,s})^{-1}Q_2^{-1}\|_\infty \quad (10)$$

which shows that  $d^Y(\hat{P}_s, P_{0,s})$  depends on the particular choices of lcf's of  $\hat{P}_s$  and  $C_s^{\text{exp}}$ . Note that  $d^Y(\hat{P}_s, P_{0,s})$  is invariant to the specific choice of rcf of  $P_{0,s}$ . Here, a normalized rcf of  $P_{0,s}$  is used with right graph symbol  $\tilde{G}_{0,s}$ .

From (10), it follows that any  $\hat{P}_s$  determined based on (9) depends on arbitrary transfer function matrices  $Q_1$  and  $Q_2$ . The key technical result of this section is the derivation of particular expressions for  $Q_1$  and  $Q_2$  such that  $d^Y(\hat{P}_s, P_{0,s})$  in (10) becomes equal to the traditional closed-loop identification criterion  $\|T(P_{0,s}, C_s^{\text{exp}}) - T(\hat{P}_s, C_s^{\text{exp}})\|_\infty$  as is used

in, e.g., [2], [22], and [31]. In particular, this constitutes Contribution C2 of this paper and provides a formal distance interpretation to the earlier obtained, that is,

$$d^Y(\hat{P}_s, P_{0,s}) = \|T(P_{0,s}, C_s^{\text{exp}}) - T(\hat{P}_s, C_s^{\text{exp}})\|_\infty. \quad (11)$$

Note that the right-hand side of (11) has a very natural interpretation. Indeed, by the application of the triangle inequality

$$\|T(P_{0,s}, C_s^{\text{exp}})\|_\infty \leq \|T(\hat{P}_s, C_s^{\text{exp}})\|_\infty + \|T(P_{0,s}, C_s^{\text{exp}}) - T(\hat{P}_s, C_s^{\text{exp}})\|_\infty$$

see [2], implies that  $\|T(P_{0,s}, C_s^{\text{exp}})\|_\infty \approx \|T(\hat{P}_s, C_s^{\text{exp}})\|_\infty$ , i.e., the closed-loop performance of  $[P_{0,s}, C_s^{\text{exp}}]$  and  $[\hat{P}_s, C_s^{\text{exp}}]$  are equal.

To proceed with the derivations, first note that [9, Sec. 1.2.3]

$$T(\hat{P}_s, C_s^{\text{exp}}) = \tilde{G}_s(\tilde{K}_s^{\text{exp}}\tilde{G}_s)^{-1}\tilde{K}_s^{\text{exp}}$$

where  $\tilde{G}_s$  is a normalized right graph symbol for  $\hat{P}_s$ , and  $\tilde{K}_s^{\text{exp}}$  is a normalized right inverse graph symbol for  $C_s^{\text{exp}}$ . Suppose that  $Q_1$  in (10) is chosen as  $Q_1 = (\tilde{G}_s\tilde{K}_s^{\text{exp}})^{-1}$ . This choice of  $Q_1$  is allowed since  $[\hat{P}_s, C_s^{\text{exp}}]$  is assumed internally stable which yields  $Q_1, Q_1^{-1} \in \mathcal{RH}_\infty$ . Then,  $\{\tilde{N}_s = Q_1\tilde{N}_s, \tilde{M}_s = Q_1\tilde{M}_s\}$  is a nonnormalized coprime factorization of  $\hat{P}_s$  with corresponding left graph symbol  $\tilde{G}_s$  given by

$$\tilde{G}_s = (\tilde{G}_s\tilde{K}_s^{\text{exp}})^{-1}\tilde{G}_s. \quad (12)$$

Next, (11) is derived in the following theorem.

*Theorem 3:* Let  $\hat{P}_s \in \mathcal{R}^{n_y \times n_u}$ ,  $P_{0,s} \in \mathcal{R}^{n_y \times n_u}$ , and  $C_s^{\text{exp}} \in \mathcal{R}^{n_u \times n_y}$  such that  $[\hat{P}_s, C_s^{\text{exp}}]$  and  $[P_{0,s}, C_s^{\text{exp}}]$  are internally stable. Let  $\{\tilde{N}_s = Q_1\tilde{N}_s, \tilde{M}_s = Q_1\tilde{M}_s\}$  be an lcf of  $\hat{P}_s$  with  $Q_1 = (\tilde{G}_s\tilde{K}_s^{\text{exp}})^{-1}$ , where  $\{\tilde{N}_s, \tilde{M}_s\}$  is a normalized lcf of  $\hat{P}_s$ . Furthermore, let  $\{\tilde{U}_s^{\text{exp}}, \tilde{V}_s^{\text{exp}}\}$  denote a normalized lcf of  $C_s^{\text{exp}}$ , i.e.,  $Q_2 = I$ . Then

$$d^Y(\hat{P}_s, P_{0,s}) = \|T(P_{0,s}, C_s^{\text{exp}}) - T(\hat{P}_s, C_s^{\text{exp}})\|_\infty.$$

*Proof:* Substituting  $Q_1 = (\tilde{G}_s\tilde{K}_s^{\text{exp}})^{-1}$  and  $Q_2 = I$  into (10)

$$\begin{aligned} d^Y(\hat{P}_s, P_{0,s}) &= \|(\tilde{G}_s\tilde{K}_s^{\text{exp}})^{-1}\tilde{G}_s\tilde{G}_{0,s}(\tilde{K}_s^{\text{exp}}\tilde{G}_{0,s})^{-1}\|_\infty \\ &= \|\tilde{K}_s^{\text{exp}}(\tilde{G}_s\tilde{K}_s^{\text{exp}})^{-1}\tilde{G}_s\tilde{G}_{0,s}(\tilde{K}_s^{\text{exp}}\tilde{G}_{0,s})^{-1}\tilde{K}_s^{\text{exp}}\|_\infty. \end{aligned} \quad (13)$$

By substituting the identity  $\tilde{K}_s^{\text{exp}}(\tilde{G}_s\tilde{K}_s^{\text{exp}})^{-1}\tilde{G}_s = I - \tilde{G}_s(\tilde{K}_s^{\text{exp}}\tilde{G}_s)^{-1}\tilde{K}_s^{\text{exp}}$  in (13), it follows that

$$\begin{aligned} d^Y(\hat{P}_s, P_{0,s}) &= \|(I - \tilde{G}_s(\tilde{K}_s^{\text{exp}}\tilde{G}_s)^{-1}\tilde{K}_s^{\text{exp}})\tilde{G}_{0,s}(\tilde{K}_s^{\text{exp}}\tilde{G}_{0,s})^{-1}\tilde{K}_s^{\text{exp}}\|_\infty \\ &= \|\tilde{G}_{0,s}(\tilde{K}_s^{\text{exp}}\tilde{G}_{0,s})^{-1}\tilde{K}_s^{\text{exp}} - \tilde{G}_s(\tilde{K}_s^{\text{exp}}\tilde{G}_s)^{-1} \times \tilde{K}_s^{\text{exp}}\|_\infty \\ &= \|T(P_{0,s}, C_s^{\text{exp}}) - T(\hat{P}_s, C_s^{\text{exp}})\|_\infty. \end{aligned}$$

□

Theorem 3 gives expressions for  $Q_1$  and  $Q_2$  such that  $d^Y(\hat{P}_s, P_{0,s})$  in (10) becomes equal to the closed-loop identification criterion  $\|T(P_{0,s}, C_s^{\text{exp}}) - T(\hat{P}_s, C_s^{\text{exp}})\|_\infty$ . This

four-block identification criterion is frequently used in the identification for control, see [2], [22], and [31], and is particularly suitable for lightly damped systems. In Section IV-B, a numerical tractable identification algorithm is proposed that exploits the distance measure  $d^Y(P_s, P_{0,s})$  as proposed in Theorem 3 to estimate a nominal model  $\hat{P}_s$ .

*Remark 1:* The presented results are related to the non-normalized coprime factorization of  $\hat{P}_s$  proposed in [18], where  $\{N_s, M_s\}$  is a rcf of  $\hat{P}_s$  with graph symbol  $G_s = \bar{G}_s(\bar{K}_s^{\text{exp}}\bar{G}_s)^{-1}$ . Similarly,  $\{N_{0,s}, M_{0,s}\}$  is a rcf of  $P_{0,s}$  with graph symbol  $G_{0,s} = \bar{G}_{0,s}(\bar{K}_{0,s}^{\text{exp}}\bar{G}_{0,s})^{-1}$ . Based on these definitions for  $G_s$  and  $G_{0,s}$ , it can be shown that

$$\|T(P_{0,s}, C_s^{\text{exp}}) - T(\hat{P}_s, C_s^{\text{exp}})\|_\infty = \|G_{0,s} - G_s\|_\infty.$$

### B. Frequency-Domain Identification Algorithm

The proposed coprime factorizations in Section IV-A lead to the following criterion for (9):

$$d^Y(\hat{P}_s, P_{0,s}) = \|\tilde{G}_s G_{0,s}\|_\infty \quad (14)$$

with  $\tilde{G}_s$  as defined in (12), and  $G_{0,s} = \bar{G}_{0,s}(\bar{K}_{0,s}^{\text{exp}}\bar{G}_{0,s})^{-1}$ . Solving (9) with criterion (14) would, however, require an infinite data set due to  $\mathcal{H}_\infty$ -norm. Therefore, an algorithm is proposed in this section to determine  $\hat{P}_s$  based on a finite set of measured frequencies.

Let a discrete frequency grid be denoted as  $\Omega = \{\omega_1, \omega_2, \dots, \omega_m\}$ , with frequency points  $\omega_i$ ,  $i = 1, 2, \dots, m$ , where  $m$  is the number of frequencies. Define  $d_\Omega^Y(\hat{P}_s, P_{0,s})$  on the discrete frequency grid  $\Omega$  as

$$d_\Omega^Y(\hat{P}_s, P_{0,s}) = \max_{\omega_i \in \Omega} \bar{\sigma}(\tilde{G}_s(j\omega_i)G_{0,s}(j\omega_i)).$$

From the frequency-domain interpretation of the  $\mathcal{H}_\infty$ -norm, it follows that  $d_\Omega^Y(\hat{P}_s, P_{0,s}) \leq d^Y(\hat{P}_s, P_{0,s})$ . This bound is, in general, tight if  $\Omega$  is chosen sufficiently dense, which can be enforced by an appropriate experiment design, see [3], [32]. Therefore, the following optimization problem with finite measurement data is proposed:

$$\min_{\hat{P}_s} d_\Omega^Y(\hat{P}_s, P_{0,s}). \quad (15)$$

To determine  $\hat{P}_s$  according to (15), three steps are presented in the remaining as follows.

- 1) *Frequency Response Function Measurements:* An approach is presented to determine a FRF of  $G_{0,s}(j\omega_i)$  based on  $T(P_{0,s}(j\omega_i), C_s^{\text{exp}}(j\omega_i))$  for  $\Omega$ .
- 2) *Model Parametrization:* A parametrization is proposed for  $\hat{P}_s$  based on matrix fraction descriptions that are particularly suited for multivariable systems.
- 3) *Identification Criterion and Algorithm:* An algorithm is proposed to solve (15).

First, an approach is described to determine the FRF of  $G_{0,s}(j\omega_i)$ .

1) *Frequency Response Function Measurements:* Let  $T(P_{0,s}(j\omega_i), C_s^{\text{exp}}(j\omega_i))$  denote a FRF measurement on the frequency grid  $\Omega$ , see [32] for further details. By using that  $T(P_{0,s}, C_s^{\text{exp}}) = \bar{G}_{0,s}(\bar{K}_{0,s}^{\text{exp}}\bar{G}_{0,s})^{-1}\bar{K}_{0,s}^{\text{exp}}$  and  $\bar{K}_{0,s}^{\text{exp}}(\bar{K}_{0,s}^{\text{exp}})^* = I$ , see [9], it directly follows that  $G_{0,s}(j\omega_i)$  can be estimated based on  $T(P_{0,s}(j\omega_i), C_s^{\text{exp}}(j\omega_i))$  according to

$$G_{0,s}(j\omega_i) = T(P_{0,s}(j\omega_i), C_s^{\text{exp}}(j\omega_i))(\bar{K}_{0,s}^{\text{exp}}(j\omega_i))^*. \quad (17)$$

2) *Model Parametrization:* A parametrization is proposed for  $\hat{P}_s$  in terms of matrix fraction descriptions, see [33] for further details. The multivariable model  $\hat{P}_s$  is represented by a polynomial left matrix fraction description  $\hat{P}_s(s, \theta) = A(s, \theta)^{-1}B(s, \theta)$ , where  $A(s, \theta) \in \mathbb{R}[s]^{n_y \times n_y}$ ,  $B(s, \theta) \in \mathbb{R}[s]^{n_y \times n_u}$ , and  $\theta$  is a real-valued parameter vector. Then, using  $\tilde{G}_s = (\bar{V}_s^{\text{exp}} - \hat{P}_s \bar{U}_s^{\text{exp}})^{-1}[I \quad -\hat{P}_s]$ , it follows that  $\tilde{G}_s(s, \theta)$  is by substituting  $\hat{P}_s(s, \theta) = A(s, \theta)^{-1}B(s, \theta)$  and rearranging terms given by

$$\tilde{G}_s(s, \theta) = R(s, \theta)[-A(s, \theta) \quad B(s, \theta)] \quad (18)$$

with  $R(s, \theta) = (B(s, \theta)\bar{U}_s^{\text{exp}}(s) - A(s, \theta)\bar{V}_s^{\text{exp}}(s))^{-1}$ . Note that the parametrization of  $\tilde{G}_s(s, \theta)$  in (18) is not unique. Alternatives include a polynomial parametrization of  $\tilde{G}_s$ , see [4, Sec. 3.3], [34], for single-input, single-output systems. The key advantage of the parametrization in (18) is that the following result holds [18, Th. 4]:  $[\hat{P}_s, C_s^{\text{exp}}]$  is internally stable if and only if  $\tilde{G}_s(s, \theta) \in \mathcal{RH}_\infty$ . As a result, only the condition  $\tilde{G}_s(s, \theta) \in \mathcal{RH}_\infty$  has to be checked to guarantee that the closed-loop system is internally stable.

3) *Identification Criterion and Algorithm:* Let  $\tilde{G}_s$  be parametrized as in (18). Then, (15) can be rewritten as the following optimization problem that aims to determine the parameters  $\theta$  of  $\hat{P}_s(s, \theta)$ :

$$\min_{\theta} \max_{\omega_i \in \Omega} \bar{\sigma}(\tilde{G}_s(j\omega_i, \theta)G_{0,s}(j\omega_i)) \quad (19)$$

based on  $\tilde{G}_s(j\omega_i, \theta)$  parametrized as in (18), and  $G_{0,s}(j\omega_i)$  in (17). Here, Lawson's algorithm [35], [36] is used to determine  $\theta$  according to (19). A comparison of methods presented in [37] showed that Lawson's algorithm results in good convergence properties and accurate solutions when used for similar identification problems as (19). The proposed algorithm employs an iterative scheme that alternates between solving a weighted least-squares problem, and adjusting the weighting used in this least-squares problem. Hence, efficient gradient-based optimization can be used to determine  $\theta$ .

For the selected parametrization of  $\tilde{G}_s$  in (20), minimizing  $V(\theta)$  in (20) is nonlinear in the parameters  $\theta$ . This nonlinearity in  $\theta$  is addressed by considering a sequence of linear least squares problems. In particular, by substituting (18) evaluated at  $\omega_i$  in (20), rearranging terms and using the identity  $\text{vec}(ABC) = (C^T \otimes A)\text{vec}(B)$  [38], (20) becomes

$$V(\theta) = \sum_{i=1}^m \|W_{ls,i}^{<k>}(j\omega_i, \theta)\text{vec}([-A(j\omega_i, \theta)B(j\omega_i, \theta)])\|_2^2 \quad (21)$$

with  $W_{ls,i}^{<k>}(j\omega_i, \theta)$  in (16), as shown at the bottom of the next page.

---

**Algorithm 1** Lawson's Algorithm
 

---

- a) Set  $\theta^0$  and  $w_i^{<k>} = \frac{1}{m}$ .  
 b) Solve  $\theta^{<k+1>} = \arg \min_{\theta} V(\theta)$ , where

$$V(\theta) = \sum_{i=1}^m \left\| \text{vec} \left( \sqrt{w_i^{<k>}} \tilde{G}_s(j\omega_i, \theta) G_{0,s}(j\omega_i) \right) \right\|_2^2 \quad (20)$$

- c) Update the weights

$$w_i^{<k+1>} = \frac{\bar{\sigma}(\tilde{G}_s(j\omega_i, \theta^{<k+1>})) G_{0,s}(j\omega_i) w_i^{<k>}}{\sum_i (\bar{\sigma}(\tilde{G}_s(j\omega_i, \theta^{<k+1>})) G_{0,s}(j\omega_i) w_i^{<k>})}$$

- d) Stop if a stopping criterion is fulfilled, otherwise set  $k = k + 1$  and go to step b).
- 

By using the parameterization in (18), minimization of  $V(\theta)$  in (21) is addressed by iteratively solving a linear least squares problem, see [36], which is a closed-loop extension of classical Sanathanan–Koerner (SK) iterations and Gauss–Newton iterations [32]. In addition, numerically reliable implementations are provided in [36] to guarantee accurate solutions and reliable convergence properties. Since the SK-algorithm used in Step b) in Algorithm 1 can result in a local optimum, global convergence of Algorithm 1 cannot be guaranteed in general. Extensive experience has shown good convergence properties, which is in line with [37].

### C. Concluding Remarks

In this section, an identification for control approach is proposed which completes Contribution C2. First, a particular choice is proposed for coprime factorizations of  $\hat{P}_s$  and  $C_s^{\text{exp}}$  such that the distance measure  $d^Y(\hat{P}_s, P_{0,s})$  is equal to a frequently used cost criterion in closed-loop system identification. Second, an identification algorithm is proposed to determine  $\hat{P}_s$  based on finite measurement data. Based on the identified  $\hat{P}_s$  and its associated value of  $d_{\Omega}^Y(\hat{P}_s, P_{0,s})$ , a controller  $C_s$  can be determined that achieves high nominal performance, while taking robust stability into consideration.

In the remaining of this paper, it is assumed that Algorithm 1 converges and that  $d_{\Omega}^Y(\hat{P}_s, P_{0,s}) = d^Y(\hat{P}_s, P_{0,s})$ . Then, the robust stability and performance conditions derived in Section III-B also hold for  $d_{\Omega}^Y(\hat{P}_s, P_{0,s})$  [instead of  $d^Y(\hat{P}_s, P_{0,s})$ ].

## V. PROPOSED IDENTIFICATION AND CONTROL PROCEDURE

The aim of the identification and control approach proposed in this paper is to design  $C_s$  such that high performance is achieved for the true plant  $P_{0,s}$ . The robust stability and performance conditions in Theorems 1 and 2 are at the

basis of the developed approach. Recall that condition (7) in Theorem 2 illustrates that the performance in terms of  $b^Y(P_{0,s}, C_s)$  is comparable to  $b^Y(\hat{P}_s, C_s)$  if  $d^Y(\hat{P}_s, P_{0,s})$  is small and the robust stability condition  $d^Y(\hat{P}_s, P_{0,s}) < b^Y(\hat{P}_s, C_s)$  holds. In view of these observations, an identification approach was presented in Section IV that aimed to determine a model  $\hat{P}_s$  such that  $d^Y(\hat{P}_s, P_{0,s})$  is minimized. In this section, a controller synthesis method is proposed that simultaneously addresses nominal performance and robust stability. Together with the identification method in Section IV, this constitutes the following identification and control approach.

---

**Procedure 1** Identification and Control Approach for the Dual-Youla Uncertainty Structure
 

---

1. **Measurements:** Determine a FRF  $T(P_0(j\omega_i), C_s^{\text{exp}}(j\omega_i))$ ,  $\omega_i \in \Omega$ ;
2. **Weighting function design:** Construct weighting functions  $W_1$  and  $W_2$  to specify performance and robustness requirements, and construct  $T(P_{0,s}(j\omega_i), C_s^{\text{exp}}(j\omega_i))$  according to

$$T(P_{0,s}, C_s^{\text{exp}}) = \begin{bmatrix} W_2 & 0 \\ 0 & W_1^{-1} \end{bmatrix} T(P_0, C_s^{\text{exp}}) \begin{bmatrix} W_2^{-1} & 0 \\ 0 & W_1 \end{bmatrix}$$

3. **Identification:** Solve the optimization problem (19) by using Algorithm 1. Let  $d_{\Omega}$  be the achieved minimum cost and  $\hat{P}_s$  a model which achieves this minimum cost;
4. **Controller synthesis:** Determine  $C_s$  based on the  $\mathcal{H}_{\infty}$ -norm minimization problem

$$\min_{C_s \text{ stabilizing}} \left\| \begin{bmatrix} d_{\Omega} \bar{K}_s (\tilde{G}_s \bar{K}_s)^{-1} & \epsilon \bar{K}_s (\tilde{G}_s \bar{K}_s)^{-1} \tilde{G}_s \end{bmatrix} \right\|_{\infty}, \quad (22)$$

with  $\tilde{G}_s$  as in (12), and  $\epsilon \in (0, 1)$  a design parameter.

5. **Verification:** Check the robust stability condition  $d_{\Omega} < b^Y(\hat{P}_s, C_s)$ . If  $d_{\Omega} \geq b^Y(\hat{P}_s, C_s)$ , change the performance specifications in  $W_1$  and  $W_2$  and repeat from Step 2.
- 

In Step 1 of Procedure 1,  $T(P_0(j\omega_i), C_s^{\text{exp}}(j\omega_i))$  is determined by means of FRF measurements,<sup>1</sup> see [32] for further details. Weighting functions are designed in Step 2 according to the procedure in [27].

In Step 3, a nominal model  $\hat{P}_s$  is determined by solving (19), with achieved cost  $d_{\Omega}$ . Then, the condition in Theorem 1 becomes

$$d_{\Omega} < b^Y(\hat{P}_s, C_s) \quad (23)$$

<sup>1</sup>Closed-loop frequency response data can also be used in iterative identification and control redesigns to invalidate a proposed controller update on the basis of loss of closed-loop stability or performance deterioration if the original controller were to be replaced by a proposed new controller [39], [40].

---


$$W_{ls,i}^{<k>}(j\omega_i, \theta) = (G_{0,s}^T(j\omega_i) \otimes \sqrt{w_i^{<k>}} (B(j\omega_i, \theta) \bar{U}_s^{\text{exp}}(j\omega_i) - A(j\omega_i, \theta) \bar{V}_s^{\text{exp}}(j\omega_i))^{-1}). \quad (16)$$

under the assumption in Section IV-B that  $d_{\Omega}^Y(\hat{P}_s, P_{0,s}) = d^Y(\hat{P}_s, P_{0,s})$ . In addition, it is noted that in practice satisfaction of this assumption may be subject to further experimental procedures. Indeed, the identified FRF in Step 1 may contain measurement noise, intergrid frequency errors, and so on. Various experimental procedures exist to quantify these errors. Depending on the experimental conditions, these errors may be considered from different perspectives. On one hand of the spectrum of approaches, a worst case perspective essentially overbounds all these error sources, potentially leading to a very conservative model set, see [9, Sec. 9.5.2]. Such an approach may be useful when only a single data set is available. On the other hand, a model validation perspective attempts to invalidate some of the irrelevant model sets, which may be very suitable if a large number of data sets is employed, otherwise, it may lead to a rather optimistic estimation of uncertainty [9, Sec. 9.5.1]. In between these extreme viewpoints, many relevant uncertainty modeling techniques have been developed, the interested reader is referred to [41]–[43] for approaches that have been developed for the same application class as is considered in this paper. Depending on which viewpoint is taken, that, of course, depends on the particular application at hand, this leads to different consequences on how these phenomena affect the bound  $d^Y(\hat{P}_s, P_{0,s})$ , as well as possible adjustment of the criterion (19) to identify the smallest model set. To anticipate, in the application in Section VI, the input will be selected such that the frequency grid is sufficiently dense and such that noise is averaged out. Hence, only the estimated FRF is needed for completing Procedure 1.

The goal of the subsequent controller synthesis based on  $\hat{P}_s$  in Step 4 of Procedure 1 is to achieve: 1) high nominal performance and 2) robust stability as precisely characterized by (23). Since  $\|\tilde{K}_s(\tilde{G}_s\tilde{K}_s)^{-1}\|_{\infty}^{-1} \leq b^Y(\hat{P}_s, C_s)$ , it can be easily seen that  $\|d_{\Omega}\tilde{K}_s(\tilde{G}_s\tilde{K}_s)^{-1}\|_{\infty} < 1$  is a sufficient condition for the robust stability condition in (23) to hold. Furthermore,  $\|\tilde{K}_s(\tilde{G}_s\tilde{K}_s)^{-1}\tilde{G}_s\|_{\infty} = \|T(\hat{P}_s, C_s)\|_{\infty}$  is a measure for nominal performance. Hence, the rationale behind the used cost function is that (22) combines robust stability and nominal performance requirements in a single-objective function. The design parameter  $\epsilon$  is used to allow for a tradeoff between both requirements. Note that the McMillan degree of  $C_s$  is bounded by the sum of the McMillan degrees of  $\hat{P}_s$  and  $C_s^{\text{exp}}$ . This is a direct consequence of the choice for a nonnormalized lcf  $\{\tilde{N}_s, \tilde{M}_s\}$  of  $\hat{P}_s$  in Section IV-A, which has a McMillan degree that is bounded by the McMillan degrees of  $\hat{P}_s$  and  $C_s^{\text{exp}}$ . In contrast, the McMillan degree of  $\tilde{G}_s$  based on a normalized lcf  $\{\tilde{N}_s, \tilde{M}_s\}$  of  $\hat{P}_s$  is bounded by the McMillan degree of  $\hat{P}_s$  [9]. As a result,  $C_s$  obtained with the proposed approach has a higher McMillan degree than for the case based on a normalized lcf of  $\hat{P}_s$ . The  $\mathcal{H}_{\infty}$ -norm minimization problem in (22) can be readily solved using the general approach proposed in [29]. Finally, in Step 5 of Procedure 1, the robustness stability condition (23) is verified, and if required, the weighting functions  $W_1$  and  $W_2$  can be changed based on engineering insight, or the weight-optimization approach used in [44] and [45].

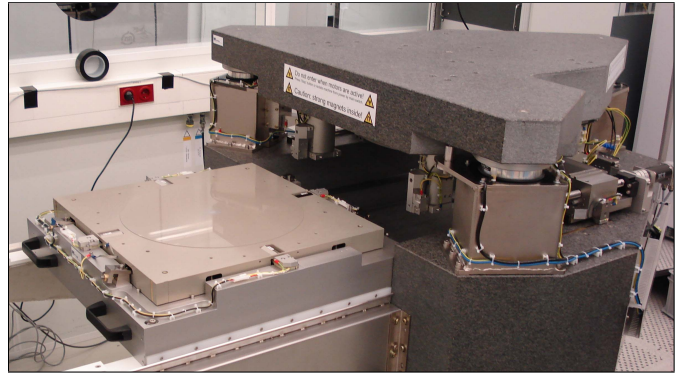


Fig. 3. Prototype industrial positioning system.

## VI. APPLICATION TO A WAFER STAGE

### A. Wafer Stage Control Design

Wafer scanners are the state-of-the-art equipment for the automated mass-production of integrated circuits (ICs). In the production process, a photoresist is exposed on a silicon disk, which is called a wafer. In this exposure, the image of the desired IC patterns is contained on a reticle, which is projected through a lens on the photoresist. Typically, more than 20 layers are required for each IC, and each wafer contains more than 200 ICs that are sequentially exposed. During this exposure task, the wafer must track an extremely accurate reference trajectory in six motion degrees of freedom. In turn, this requires the design of a high-performance feedback controller.

In this paper, the feedback control design for the prototype industrial positioning system depicted in Fig. 3 is considered. Traditionally, the feedback control design of such systems is performed through manual loop-shaping [46]. In view of increasing requirements, a systematic model-based approach is promising, e.g., [43], [47]. Interestingly, model-based approaches that involve an  $\mathcal{H}_{\infty}$ -norm have been most successful for a number of reasons, including their natural connection to loop-shaping [9]. Indeed, typical performance is specified through specification of the closed-loop bandwidth, defined as a crossover frequency. This performance is limited by a performance-robustness tradeoff, as is clearly exemplified in [48, Sec. 3], where it is also shown that  $\mathcal{H}_{\infty}$ -loop-shaping offers a very natural framework for wafer stage motion control design.

The wafer stage in Fig. 3 is designed to be lightweight and includes an additional number of actuators and sensors to actively control flexible dynamical behavior [48], which is in sharp contrast to traditional mechatronic system designs [49], [50]. The system is controlled in all six motion degrees-of-freedom (DOF) (i.e., three rotations and three translations). The actuators are Lorentz motors, whereas the measurement system consists of three linear incremental encoders with a resolution of 1 nm in the vertical plane in addition to capacitive sensors in the horizontal plane. In this paper, Procedure 1 is applied to a single translational DOF in the horizontal plane to show the potential of nonnormalized coprime factorizations.

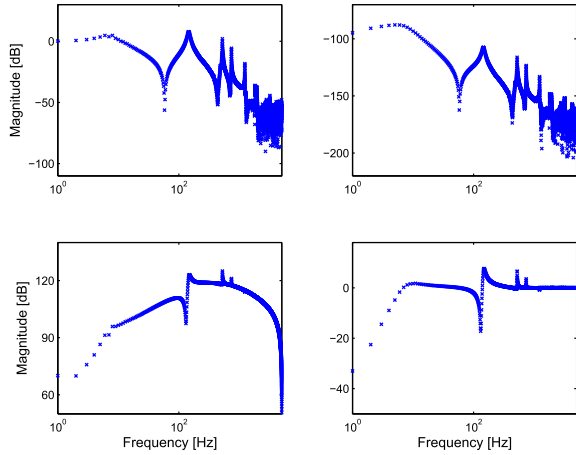


Fig. 4. Identified FRF of the closed-loop system  $T(P_0, C_s^{\text{exp}})$  for  $\omega_i \in \Omega_{id}$ .

### B. Application of Procedure 1

1) *Step 1*: A stabilizing controller  $C_s^{\text{exp}}$  is given that achieves a crossover frequency of 10 Hz. A closed-loop identification experiment is performed to obtain the FRF  $T(P_0(j\omega_i), C_s^{\text{exp}}(j\omega_i))$ ,  $\omega_i \in \Omega_{id}$ , as depicted in Fig. 4. Here, multisine experiments are performed as is explained in [43, Appendix A]. The main advantage is that the noise error is rendered negligible by increasing the experiment length. In addition, a dense frequency grid is chosen such that intergrid interpolation errors can be neglected [42].

2) *Step 2*: Then, in Step 2 of Procedure 1, weighting filters are selected in view of the loop-shaping paradigm. Irrespective of the different nonnormalized coprime factorization-based approach developed in this paper to represent model uncertainty, the weighting filters can be either manually chosen as indicated in [27] or obtained via optimization methods as described in [44], [52], and [53], see also [53, Sec. 2A] for an application to wafer stage motion control. In particular, the weighting functions

$$W_1(s) = 1, \quad W_2(s) = \frac{8.883 \times 10^5 s + 3.349 \times 10^7}{s^3 + 754s^2 + 8.883 \times 10^5 s} \quad (24)$$

are considered. This selection aims at a target crossover frequency of 30 Hz, and specifying integral action and controller rolloff in the low-frequency and high-frequency range, respectively. Indeed, the reference in wafer stage motion control typically has low-frequency content. This particular weighting filter choice thus implies that good reference tracking is achieved at low frequencies, i.e., below 30 Hz. In addition, it avoids the amplification of measurement noise above the crossover frequency of 30 Hz, which is a well-known tradeoff in feedback design, and clearly observed in loop-shaping-based designs [26, Ch. 9]. Based on this design,  $T(P_{0,s}(j\omega_i), C_s^{\text{exp}}(j\omega_i))$  is now constructed.

3) *Step 3*: In Step 3 of Procedure 1, a 10th-order nominal model  $\hat{P}_s$  is identified by using Algorithm 1 based on the FRF  $T(P_{0,s}(j\omega_i), C_s^{\text{exp}}(j\omega_i))$ ,  $\omega_i \in \Omega_{id}$ . Three iterations of Algorithm 1 were required to converge to a stationary point. Since the condition  $\tilde{G}_s(s, \theta) \in \mathcal{RH}_\infty$  holds, it follows that  $[\hat{P}_s, C_s^{\text{exp}}]$  is internally stable and that  $\{\tilde{N}_s, \tilde{M}_s\}$  is a lcf of  $\hat{P}_s$ .

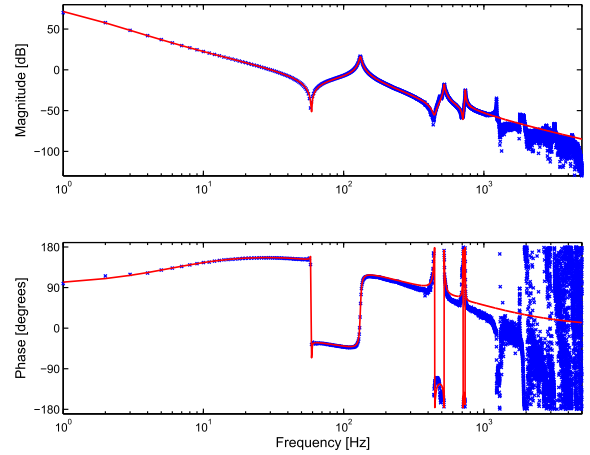


Fig. 5. FRF of the true plant  $P_{0,s}$  for  $\omega_i \in \Omega_{id}$  (blue dotted) and 10th-order parametric model  $\hat{P}_s$  (red solid).

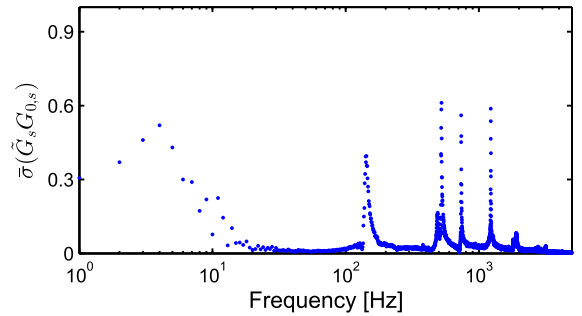


Fig. 6. Identification criterion  $\bar{\sigma}(\tilde{G}_s G_{0,s})$ ,  $\omega_i \in \Omega_{id}$ .

The identified model  $\hat{P}_s = \tilde{M}_s^{-1} \tilde{N}_s$  is depicted in Fig. 5, and it can be seen to very accurately describe the true plant's rigid-body behavior and three resonance phenomena. That is, the proposed identification procedure automatically yields a good fit around the target crossover frequency of 30 Hz. Resonance phenomena in the high-frequency range are not modeled in  $\hat{P}_s$ . Essentially, these dynamics are not important for robust stability due to rolloff in the high-frequency range as specified in  $W_2$ . This is confirmed in Fig. 6, which shows that the identification criterion  $\bar{\sigma}(\tilde{G}_s(j\omega_i)G_{0,s}(j\omega_i))$  has dominant contributions for the first three resonance phenomena, which are, therefore, included in  $\hat{P}_s$ . The achieved minimum cost of the identification algorithm is given by  $d_\Omega = 0.6113$ .

4) *Step 4*: In Step 4 of Procedure 1,  $C_s$  is determined according to (22) with  $d_\Omega = 0.6113$  and design parameter  $\epsilon = 0.5$ .

5) *Step 5*: The resulting controller  $C_s$  achieves a nominal performance of  $\|T(\hat{P}_s, C_s)\|_\infty = 5.5932$ . By using a robust stability condition in the  $\mathcal{H}_\infty$  minimization problem in (22), the robust stability margin for  $C_s$  becomes  $b^Y(\hat{P}_s, C_s) = 0.6473$ , which implies that  $[P_{0,s}, C_s]$  is guaranteed to be internally stable since  $d_\Omega = 0.6113$ . Finally, note that  $\|T(\hat{P}_s, C_s^{\text{exp}})\|_\infty = 79.4801$ , confirming that  $C_s$  significantly improves performance for the considered mechanical system with lightly damped poles and zeros compared to the preexisting controller  $C_s^{\text{exp}}$ . In particular, a small value of  $\|T(\hat{P}_s, C_s)\|_\infty$  implies that the desired loop-shape, specified by (24), is closely matched, whereas a large value implies a

large discrepancy, see [54] for a theoretical justification. The achieved performance can be further improved by repeating Procedure 1 with  $C_s$  as initial controller.

### C. Comparison and Discussion

To appreciate the importance of nonnormalized factorizations, the proposed approach is compared to the  $\mathcal{H}_\infty$  loop-shaping approach in [10] which employs normalized coprime factorizations. The controller resulting using these normalized coprime factorizations is referred to as  $C_s^\infty$ . First, note that due to the specific criterion (22), the  $\mathcal{H}_\infty$  loop-shaping achieves improved nominal performance, i.e.,  $\|T(\hat{P}_s, C_s^\infty)\|_\infty = 3.1390$ , compared to the nominal performance for  $\|T(\hat{P}_s, C_s)\|_\infty = 5.5932$ . However, for  $C_s^\infty$ , it holds that  $b^Y(\hat{P}_s, C_s^\infty) = 0.3456$ , and since  $0.6113 = d_\Omega > b^Y(\hat{P}_s, C_s^\infty)$ , internal stability of  $[P_{0,s}, C_s^\infty]$  cannot be guaranteed. As a result, the  $\mathcal{H}_\infty$  loop-shaping approach does not deliver a controller that is guaranteed to stabilize the true system, while the use of nonnormalized coprime factorizations has delivered a controller that is robustly stable and achieves good performance. This illustrates the advantages of the proposed approach compared to the  $\mathcal{H}_\infty$  loop-shaping approach in [10]. These results corroborate the earlier results on nonnormalized coprime factorizations from an uncertainty modeling perspective, see [18] for details.

Furthermore, when comparing to earlier robust controller designs, these typically employ  $\mu$ -synthesis. Although this is a conceptually systematic approach, the involved optimization is nonconvex and requires a substantial computational load, in addition to an excessively high order of the resulting controller, see [47], [24] for wafer stage motion control results. Although this is substantially improved by also using nonnormalized coprime factorizations, see [18], the presented approach in this paper completely avoids these difficulties.

## VII. CONCLUSION

In this paper, an identification and control procedure is developed within the general distance measure framework. In particular, results are derived for the dual-Youla uncertainty structure, as is commonly used in identification for control. First, a particular nonnormalized coprime factorization of  $\hat{P}_s$  is introduced to connect the general distance measure for a dual-Youla uncertainty structure to a closed-loop identification criterion. Second, a frequency domain identification algorithm is proposed to determine  $\hat{P}_s$ . Third, a controller  $C_s$  is determined according to a  $\mathcal{H}_\infty$  minimization problem with an objective function that addresses nominal performance and robust stability requirements. An experimental example of a mechanical system with lightly damped poles and zeros demonstrates the use of the proposed identification and control approach and confirms the advantages of the proposed approach for such systems.

Future work includes an extension of the proposed framework to other uncertainty structures in the distance measure framework of [12], the use of the developed distance measures for model reduction, and an application to multivariable systems with lightly damped poles and zeros.

## REFERENCES

- [1] S. Garatti, M. C. Campi, and S. Bittanti, "Iterative robust control: Speeding up improvement through iterations," *Syst. Control Lett.*, vol. 59, no. 2, pp. 139–146, 2010.
- [2] R. J. P. Schrama, "Accurate identification for control: The necessity of an iterative scheme," *IEEE Trans. Autom. Control*, vol. 37, no. 7, pp. 991–994, Jul. 1992.
- [3] H. Hjalmarsson, "From experiment design to closed-loop control," *Automatica*, vol. 41, no. 3, pp. 393–438, Mar. 2005.
- [4] P. Date and A. Lanzon, "A combined iterative scheme for identification and control redesigns," *Int. J. Adapt. Control Signal Process.*, vol. 18, no. 8, pp. 629–644, 2004.
- [5] A. Lecchini, A. Lanzon, and B. D. O. Anderson, "A model reference approach to safe controller changes in iterative identification and control," *Automatica*, vol. 42, no. 2, pp. 193–203, 2006.
- [6] M. Vidyasagar, "The graph metric for unstable plants and robustness estimates for feedback stability," *IEEE Trans. Autom. Control*, vol. AC-29, no. 5, pp. 403–418, May 1984.
- [7] A. El-Sakkary, "The gap metric: Robustness of stabilization of feedback systems," *IEEE Trans. Autom. Control*, vol. AC-30, no. 3, pp. 240–247, Mar. 1985.
- [8] T. T. Georgiou and M. C. Smith, "Optimal robustness in the gap metric," *IEEE Trans. Autom. Control*, vol. 35, no. 6, pp. 673–686, Jun. 1990.
- [9] G. Vinnicombe, *Uncertainty and Feedback, H Loop-Shaping and the V-Gap Metric*. London, U.K.: Imperial College Press, 2001.
- [10] K. Glover and D. McFarlane, "Robust stabilization of normalized coprime factor plant descriptions with  $\mathcal{H}_\infty$ -bounded uncertainty," *IEEE Trans. Autom. Control*, vol. 34, no. 8, pp. 821–830, Aug. 1989.
- [11] K. K. Chen and C. W. Rowley, "Normalized coprime robust stability and performance guarantees for reduced-order controllers," *IEEE Trans. Autom. Control*, vol. 58, no. 4, pp. 1068–1073, Apr. 2013.
- [12] A. Lanzon and G. Papageorgiou, "Distance measures for uncertain linear systems: A general theory," *IEEE Trans. Autom. Control*, vol. 54, no. 7, pp. 1532–1547, Jul. 2009.
- [13] G. C. Hsieh and M. G. Safonov, "Conservatism of the gap metric," *IEEE Trans. Autom. Control*, vol. 38, no. 4, pp. 594–598, Apr. 1993.
- [14] R. S. Smith, C.-C. Chu, and J. L. Fanson, "The design of  $\mathcal{H}_\infty$  controllers for an experimental non-collocated flexible structure problem," *IEEE Trans. Control Syst. Technol.*, vol. 2, no. 2, pp. 101–109, Jun. 1994.
- [15] B. Boulet, B. A. Francis, P. C. Hughes, and T. Hong, "Uncertainty modeling and experiments in  $\mathcal{H}_\infty$  control of large flexible space structures," *IEEE Trans. Control Syst. Technol.*, vol. 5, no. 5, pp. 504–519, Sep. 1997.
- [16] G. J. Balas and J. C. Doyle, "Control of lightly damped, flexible modes in the controller crossover region," *J. Guid., Control, Dyn.*, vol. 17, no. 2, pp. 370–377, 1994.
- [17] S. Engelken and A. Lanzon, "Revisiting robust stabilization of coprime factors: The general case," in *Proc. IEEE 51st Conf. Decis. Control*, Maui, HI, USA, Dec. 2012, pp. 1542–1547.
- [18] T. Oomen and O. Bosgra, "System identification for achieving robust performance," *Automatica*, vol. 48, no. 9, pp. 1975–1987, 2012.
- [19] S. Engelken, A. Lanzon, and S. Patra, "Robustness analysis and controller synthesis with non-normalized coprime factor uncertainty characterisation," in *Proc. 50th Conf. Decis. Control, Eur. Control Conf.*, Orlando, FL, USA, Dec. 2011, pp. 4201–4206.
- [20] M. Gevers, "Identification for control: From the early achievements to the revival of experiment design," *Eur. J. Control*, vol. 11, nos. 4–5, pp. 335–352, 2005.
- [21] T. Zhou, "Frequency response estimation for NCFs of an MIMO plant from closed-loop time-domain experimental data," *IEEE Trans. Autom. Control*, vol. 51, no. 1, pp. 38–51, Jan. 2006.
- [22] M. Gevers, "Towards a joint design of identification and control?" in *Essays on Control: Perspectives in the Theory and its Applications*. Boston, MA, USA: Birkhäuser Verlag, 1993, ch. 5, pp. 111–151.
- [23] G. Gu, "Modeling of normalized coprime factors with  $\mu$ -metric uncertainty," *IEEE Trans. Autom. Control*, vol. 44, no. 8, pp. 1498–1511, Aug. 1999.
- [24] R. A. de Callafon and P. M. J. Van Den Hof, "Suboptimal feedback control by a scheme of iterative identification and control design," *Math. Model. Syst.*, vol. 3, no. 1, pp. 77–101, 1997.
- [25] S. G. Douma and P. M. J. Van den Hof, "Relations between uncertainty structures in identification for robust control," *Automatica*, vol. 41, no. 3, pp. 439–457, 2005.
- [26] S. Skogestad and I. Postlethwaite, *Multivariable Feedback Control: Analysis and Design*, 2nd ed. Hoboken, NJ, USA: Wiley, 2005.

- [27] D. McFarlane and K. Glover, "A loop-shaping design procedure using  $\mathcal{H}_\infty$  synthesis," *IEEE Trans. Autom. Control*, vol. 37, no. 6, pp. 759–769, Jun. 1992.
- [28] A. Lanzon, S. Engelken, S. Patra, and G. Papageorgiou, "Robust stability and performance analysis for uncertain linear systems—The distance measure approach," *Int. J. Robust Nonlinear Control*, vol. 22, no. 11, pp. 1270–1292, 2012.
- [29] K. Zhou, J. C. Doyle, and K. Glover, *Robust and Optimal Control*. Upper Saddle River, NJ, USA: Prentice Hall, 1996.
- [30] B. D. O. Anderson, "From Youla–Kucera to identification, adaptive and nonlinear control," *Automatica*, vol. 34, no. 12, pp. 1485–1506, 1998.
- [31] P. Albertos and A. P. Sala, *Iterative Identification and Control*. London, U.K.: Springer-Verlag, 2002.
- [32] R. Pintelon and J. Schoukens, *System Identification: A Frequency Domain Approach*, 2nd ed. Hoboken, NJ, USA: Wiley, 2012.
- [33] T. Kailath, *Linear Systems*. Englewood Cliffs, NJ, USA: Prentice-Hall, 1980.
- [34] P. Date and G. Vinnicombe, "Algorithms for worst case identification in  $\mathcal{H}_\infty$  and in the  $v$ -gap metric," *Automatica*, vol. 40, no. 6, pp. 995–1002, 2004.
- [35] J. R. Rice and K. H. Usow, "The Lawson algorithm and extensions," *Math. Comput.*, vol. 22, no. 101, pp. 118–127, 1968.
- [36] T. Oomen and M. Steinbuch, *Control-Oriented Modelling and Identification: Theory and Practice*. Edison, NJ, USA: IET, 2015, ch. 5, pp. 101–124.
- [37] C. Bohn and H. Unbehauen, "Minmax and least squares multivariable transfer function curve fitting: Error criteria, algorithms and comparisons," in *Proc. Amer. Control Conf.*, Philadelphia, PA, USA, Jun. 1998, pp. 3189–3193.
- [38] J. W. Brewer, "Kronecker products and matrix calculus in system theory," *IEEE Trans. Circuits Syst.*, vol. CAS-25, no. 9, pp. 772–781, Sep. 1978.
- [39] A. Dehghani, A. Lecchini-Visintini, A. Lanzon, and B. D. O. Anderson, "Validating controllers for internal stability utilizing closed-loop data," *IEEE Trans. Autom. Control*, vol. 54, no. 11, pp. 2719–2725, Nov. 2009.
- [40] S. Patra and A. Lanzon, "A closed-loop data based test for robust performance improvement in iterative identification and control redesigns," *Automatica*, vol. 48, no. 10, pp. 2710–2716, 2012.
- [41] D. K. de Vries and P. M. J. van den Hof, "Quantification of uncertainty in transfer function estimation: A mixed probabilistic-worst-case approach," *Automatica*, vol. 31, no. 4, pp. 543–557, 1995.
- [42] E. Geerardyn and T. Oomen, "A local rational model approach for  $\mathcal{H}_\infty$  norm estimation: With application to an active vibration isolation system," *Control Eng. Pract.*, vol. 68, pp. 63–70, Nov. 2017.
- [43] T. Oomen, R. van der Maas, C. R. Rojas, and H. Hjalmarsson, "Iterative data-driven  $\mathcal{H}_\infty$  norm estimation of multivariable systems with application to robust active vibration isolation," *IEEE Trans. Control Syst. Technol.*, vol. 22, no. 6, pp. 2247–2260, Nov. 2014.
- [44] A. Lanzon, "Weight optimisation in  $\mathcal{H}_\infty$  loop-shaping," *Automatica*, vol. 41, no. 7, pp. 1201–1208, 2005.
- [45] M. Osinuga, S. Patra, and A. Lanzon, "An iterative algorithm for maximizing robust performance in  $\mathcal{H}_\infty$  loop-shaping design," *Int. J. Robust Nonlinear Control*, vol. 23, no. 8, pp. 919–931, 2013.
- [46] T. Oomen, "Advanced motion control for precision mechatronics: Control, identification, and learning of complex systems," *IEEE Trans. Ind. Appl.*, vol. 7, no. 2, pp. 127–140, 2018.
- [47] M. van de Wal, G. van Baars, F. Sperling, and O. Bosgra, "Multivariable  $\mathcal{H}_\infty/\mu$  feedback control design for high-precision wafer stage motion," *Control Eng. Pract.*, vol. 10, no. 7, pp. 739–755, Jul. 2002.
- [48] R. van Herpen, T. Oomen, E. Kikken, M. van de Wal, W. Aangenent, and M. Steinbuch, "Exploiting additional actuators and sensors for nano-positioning robust motion control," *Mechatronics*, vol. 24, no. 6, pp. 619–631, 2014.
- [49] M. Li, Y. Zhu, K. Yang, and C. Hu, "A data-driven variable-gain control strategy for an ultra-precision wafer stage with accelerated iterative parameter tuning," *IEEE Trans. Ind. Informat.*, vol. 11, no. 5, pp. 1179–1189, Oct. 2015.
- [50] J. Bolder, J. van Zundert, S. Koekebakker, and T. Oomen, "Enhancing flatbed printer accuracy and throughput: Optimal rational feedforward controller tuning via iterative learning control," *IEEE Trans. Ind. Electron.*, vol. 64, no. 5, pp. 4207–4216, May 2017.
- [51] M. Osinuga, S. Patra, and A. Lanzon, "Smooth weight optimization in  $\mathcal{H}_\infty$  loop-shaping design," *Syst. Control Lett.*, vol. 59, no. 11, pp. 663–670, 2010.
- [52] M. Osinuga, S. Patra, and A. Lanzon, "State-space solution to weight optimization problem in  $\mathcal{H}_\infty$  loop-shaping control," *Automatica*, vol. 48, no. 3, pp. 505–513, 2012.
- [53] F. Boeren, R. van Herpen, T. Oomen, M. van de Wal, and M. Steinbuch, "Non-diagonal  $\mathcal{H}_\infty$  weighting function design: Exploiting spatio-temporal deformations in precision motion control," *Control Eng. Pract.*, vol. 35, pp. 35–42, Feb. 2015.
- [54] D. C. McFarlane and K. Glover, *Robust Controller Design Using Normalized Coprime Factor Plant Descriptions* (Lecture Notes in Control and Information Sciences), vol. 138. Berlin, Germany: Springer-Verlag, 1990.



**Frank Boeren** received the M.Sc. (*cum laude*) and Ph.D. degrees in mechanical engineering from the Eindhoven University of Technology, Eindhoven, The Netherlands, in 2012 and 2016, respectively.

His current research interests include system identification for feedforward and feedback control, learning control, and applications in semiconductor equipment.

Dr. Boeren was a recipient of the Ph.D. Best Thesis Award in Systems and Control, which was granted by the Dutch Institute of Systems and Control, and the KIVI-NIRIA (Royal Dutch Institution of Engineers) Graduation Award for the best M.Sc. thesis in mechanical engineering.



**Alexander Lanzon** received the B.Eng.(Hons.) degree in electrical and electronic engineering from the University of Malta, Msida, Malta, in 1995, and the M.Phil. degree in robot control and the Ph.D. degree in control engineering from the University of Cambridge, Cambridge, U.K., in 1997 and 2000, respectively.

He held academic positions with Georgia Institute of Technology, Atlanta, GA, USA, and the Australian National University, Canberra, ACT, Australia, and industrial positions with ST-Microelectronics (Malta) Ltd., Kirkop, Malta; Yaskawa Denki (Tokyo) Ltd., Saitama-Ken, Japan; and National ICT Australia Ltd., Canberra, ACT, Australia. In 2006, he joined the University of Manchester, Manchester, U.K., where he now holds the Chair in Control Engineering. His current research interests include the fundamentals of feedback control theory, negative imaginary systems theory,  $\mathcal{H}_\infty$  control theory, robust linear and nonlinear feedback control systems, and applying robust control theory to innovative mechatronic, robotic, and drone applications.

Prof. Lanzon is a Fellow of the Institute of Mathematics and its Applications, the Institute of Measurement and Control and the Institution of Engineering and Technology. He is an Associate Editor of the IEEE TRANSACTIONS ON AUTOMATIC CONTROL. He has served as a Subject Editor for the *International Journal of Robust and Nonlinear Control*.



**Tom Oomen** received the M.Sc. (*cum laude*) and the Ph.D. degree from the Eindhoven University of Technology, Eindhoven, The Netherlands.

He held visiting positions with KTH, Stockholm, Sweden, and The University of Newcastle, Australia, Callaghan, NSW, Australia. He is currently an Associate Professor with the Department of Mechanical Engineering, Eindhoven University of Technology. His current research interests include system identification, robust control, and learning control, with applications in mechatronic systems.

Dr. Oomen was a recipient of the Corus Young Talent Graduation Award, the 2015 IEEE TRANSACTIONS ON CONTROL SYSTEMS TECHNOLOGY Outstanding Paper Award, and the 2017 IFAC Mechatronics Best Paper Award. He is an Associate Editor of IEEE CONTROL SYSTEMS LETTERS and IFAC Mechatronics.